SCATTERING OF ULTRASONIC WAVE ON A MODEL
OF THE ARTERY

J. WÓJCIK, T. POWAŁOWSKI, R. TYMKIEWICZ
A. LAMERS, Z. TRAWIŃSKI

Institute of Fundamental Technological Research
Polish Academy of Sciences
Świętokrzyska 21, 00-049 Warszawa, Poland
e-mail: jwojcik@ippt.gov.pl

The study was aimed at elaboration of a mathematical model to describe the process of acoustic wave propagation in an inhomogeneous and absorbing medium, whereas the wave is generated by an ultrasonic probe. The modelling process covered the phenomenon of ultrasonic wave backscattering on an elastic pipe with dimensions similar to the artery section. Later on, the numerical codes were determined in order to calculate the fields of ultrasonic waves, as well as backscattered fields for various boundary conditions. Numerical calculations make it possible to define the waveforms for electric signals that are produced when ultrasonic waves, being reflected and backscattered by an artery model, are then received by the ultrasonic probe. It is the signal which pretty well corresponds with the actual RF signal that is obtained during measurements at the output of an ultrasonic apparatus.

Key words: ultrasound, backscattering, artery, numerical model

1. Introduction

The pathological process of atherosclerosis development and its connection with alterations that occur in walls of blood vessels present a matter of interest for numerous scientific and clinical centres worldwide. Changes of elastic properties of blood vessels are considered as one of the factors that are used in non-invasive investigations to evaluate alterations that take place in vessel walls. It is why investigation of elastic properties of blood vessel walls by means of ultrasonic methods is the subject of numerous research reports that have been published in the recent years. In case of non-invasive investigations, the ultrasonic measurements for momentary diameters of arteries over the entire cardiac cycle serve as the basis enabling to determine elasticity of arterial walls. Maximum and minimum values for the vessel diameter are associated with respective systolic and diastolic blood pressures measured by a sphygmomanometer. Based on

the above measurements, a series of further elasticity factors are determined, including elasticity module E_p, [1, 2], compliance coefficient CC [3], distensibility coefficient DC [4], stiffness coefficients α [5] and β [6] and relative variation of artery diameter $\Delta D/D$ [3, 5].

In case of non-invasive ultrasonic measurement, reproducibility of the obtained results is an extremely important parameter, since it is used to define sensitivity of the diagnostic tool [7]. Reproducibility of measurements during the elasticity examination of arterial walls substantially depends on the shape of an ultrasonic beam, as well as its orientation with respect to the blood vessel. It is the problem that has not been solved yet in the theoretical way. However, solving the above problem will present an essential practical importance for the design of ultrasonic probes that are used for investigation of elasticity of various arteries, with various diameters and disposed at various depths with regard to the skin surface, e.g. the common carotid artery, the abdominal aorta or the femoral artery.

The major objective of the thesis was to develop a mathematical model that would be capable of describing spatial and time-dependent distribution of an ultrasonic beam that is emitted by a piezoelectric ring transducer and then backscattered on cylindrical surfaces of the walls in artery models. The adopted model assumes that the backscattered ultrasonic wave is received by a probe and the energy of wave is converted into electrical pulses that carry information on location of walls in the artery model. The developed model was tested for results of experiments when an elastic pipe was immersed in water. The investigations were carried out using the VED equipment, designed and constructed in the Ultrasonic Department of the Institute of Fundamental Technological Research of the Polish Academy of Sciences, purposefully dedicated for elasticity examination of arterial walls in human body.

2. Physical model

2.1. Basic equations

On using the nondimensional variables, the equation that describes the propagation of sonic wave in a homogeneous (with undisturbed parameters of the material), nonlinear and absorbing medium, can be expressed by the following equation [8–10]:

$$
\begin{aligned}
\Delta P - \partial_{tt}P - 2\partial_t \mathbf{A}P + q\beta\,\partial_{tt}(P)^2 &= 0, \\
\mathbf{A}P \equiv A(t) \otimes P(\mathbf{x},t), \qquad A(t) &= F^{-1}[a(n)],
\end{aligned}
\tag{1}
$$

where $P(\mathbf{x}, t)$ is the pressure in the 3D coordinate system $\mathbf{x}$ at the moment of time t; $\mathbf{A}$ is a convolution-type operator that defines absorption; q is the Mach number (in our case the Mach number is calculated for velocities on the surface of the disturbance); $\beta \equiv (\gamma+1)/2$; $\gamma \equiv (B/A)+1$ or γ – adiabatic exponent, $n \equiv f/f_0$ – nondimensional frequency; f, f_0 – respectively: frequency and characteristic frequency; $a(n)$ – the small signal coefficient of absorption, $\mathbf{A} = F^{-1}[a(n)]$, $F[\cdot]$ – Fourier transform.

2.2. Equation for inhomogeneous medium

For a medium, where areas with disturbed parameters of the wave-carrying material occur (e.g. with values that differ from the ones for the entire wave propagation area or due to "inclusion" of admixtures with such material properties that are different than the ones of the surrounding medium), Eq. (1) can be expressed in the following manner:

$$\Delta P - \partial_{tt} P - 2\partial_t \mathbf{A} P + q\beta \partial_{tt}(P)^2 = -\Pi \partial_{tt} P + \Gamma q\beta \partial_{tt}(P)^2,$$

$$\Pi(\mathbf{x}) \equiv 1 - \frac{1}{c_r^2}, \qquad \Gamma(\mathbf{x}) \equiv 1 - \frac{\beta_r}{g_r c_r^4},$$

(2)

where $c_r(\mathbf{x}) \equiv c_1(\mathbf{x})/c$, $g_r \equiv g_1/g$, $\beta_r \equiv \beta_1/\beta = (\gamma_1+1)/(\gamma+1)$. Respectively, c_1, g_1 and γ_1 stand for sound velocity, density and "adiabatic exponent" within the disturbed area. In our case, $c = 1$ denotes the dimensionless sound velocity in the surrounding reference medium, e.g. in water.

Equation (2) neglects perturbations $\delta\mathbf{A} \equiv \mathbf{A}_1 - \mathbf{A} = F^{-1}[a_1(n) - a(n)]$ since the algorithm that was developed by us makes it possible to achieve uniform solutions (in terms of absorption) of the model equations for all possible values of absorption and spatial configuration of absorbing constituents that have any importance for us. The Π and Γ factors may be defined as backscattering potentials: linear Π and nonlinear Γ.

2.3. Derivation of model equations for the issues of backscattering

For derivation of the equations for our model we make the following assumptions:

1. The term that is proportional to Γ describes the phenomenon of nonlinear backscattering and nonlinear propagation in the areas where medium parameters are disturbed. For cases that are important for our considerations the following relationship is fulfilled:

$$q\Gamma/\Pi \ll 1.$$

(3)

Therefore the last term in Eq. (2) can be neglected. The attention should be paid to the fact that coincidence of $c_r(\mathbf{x}) \cong 1$ and $g_r \cong 1$, i.e. practical absence of linear reflection, cannot be excluded, especially for biological substances. Mutual relationships between the phenomena of nonlinear and linear reflections are discussed in [9].

2. Generation of scanning pulses and detection of the corresponding backscattered field (echo) is a typical approach in ultrasonic diagnostic techniques. Consequently, the following distribution of the acoustic field can be applied:

$$P = P^{\mathrm{in}} + P^{\mathrm{sc}},$$

(4)

where P^{in} corresponds to the incident field whilst P^{sc} is the backscattered field. The assumption is made that P^{in} fulfils the Eq. (1).

3. Substitution of (4) into Eq. (2) leads to the terms that depend on $P^{\mathrm{in}} \cdot P^{\mathrm{sc}}$, therefore determine nonlinear "cross" effects, connected with mutual intersection and interaction of the incident field P^{in} with the backscattered field P^{sc}, either in the area

with non-disturbed parameters (the last component on the left-hand side in Eq. (2)) or, analogically, in the boundary area and in the area of disturbed parameters (the last component on the right-hand side in Eq. (2)). If scanning pulses are short, the contribution of cross-sectional phenomena to overall propagation-related nonlinear phenomena can be omitted, since the time interval when a non-zero value of the product $P^{\text{in}} \cdot P^{\text{sc}}$ exists is negligibly short as compared to the duration of the P^{in^2} field. Cumulation of nonlinear effects is a characteristic feature of the phenomena described by Eq. (1), e.g. increasing deformation of pulses waveforms leads to extension of the Fourier spectrum. Consequently, the conclusion can be made that in case of very short time intervals for interactions or propagation, the nonlinear phenomena can be also omitted. Last but not least, in spite of all the foregoing deliberations, the assumption can be made that a subsequent scanning pulse is emitted only if the response (echo) of the preceding one has been received.

For all the cases that have any importance for our considerations the assumption can be made:

$$P^{\text{in}} \cdot P^{\text{sc}} = 0. \tag{5}$$

In case of insignificant differences of material parameters for the surrounding medium and the target, pressure in the backscattered field is much lower than the pressure of incident pulses $P^{\text{sc}} \ll P^{\text{in}}$. Hence the assumption that nonlinear phenomena can be neglected for propagation of backscattered fields is absolutely justified. It must be mentioned that even these probes that are used for ultrasonography and specified as broadband are actually of the narrow-band type, as compared to the requirements related to nonlinear propagation of scanning of backscattered pulses. Notwithstanding the fact that propagation of the backscattered signal can be really nonlinear, no phenomenon related to such nonlinear propagation has been detected. Therefore we can assume that in Eq. (2)

$$qP^{\text{sc}2} = 0. \tag{6}$$

Taking into account the foregoing assumptions of Eq. (2), the following formula can be obtained to define the backscattered fields

$$\Delta P^{\text{sc}} - \partial_{tt} P^{\text{sc}} - 2\partial_t \mathbf{A} P^{\text{sc}} = -\Pi \partial_{tt}(P^{\text{sc}} + P^{\text{in}}), \tag{7}$$

where the incident field P^{in} fulfils the equation:

$$\Delta P^{\text{in}} - \partial_{tt} P^{\text{in}} - 2\partial_t \mathbf{A} P^{\text{in}} + q\beta \partial_{tt}(P^{\text{in}})^2 = 0. \tag{8}$$

The only nonlinear equation is the one numbered (8) and it determines propagation of the scanning pulses. However, if the excitation level is low, that equation can be linearized as well by omitting the last component. Equations (7) and (8) represent our mathematical model for physical phenomena that take place in the areas of propagation and backscattering of ultrasonic signals.

3. Solver

Construction of a solver for backscattered fields is the fundamental issue for setting up a numerical model of an experiment that is aimed at reflecting real situations that occur in ultrasonographic practice. The solver that we have constructed is composed of three parts:

1. Solver for the incident field. It is the solver that is based on codes JWNUT2D and JWNUT3D, which we have been using for many years. The first code solves Eq. (8) in the axially symmetrical cases, the second one is applicable to any one-sided boundary conditions (see Eq. (4)).

2. Solver for the backscattered field. It is the tool that is capable of calculating the parameters of back-scattered fields and their pressures on the detector surface, whereas the tool uses the numerically determined incident field and information on geometrical and material parameters of the target as the basis for calculations.

3. Simulator of the electronic receiver channel that is used for calculation of pulse responds $h(t)$ of this unit. Distribution of pressure on the surface of the probe is averaged over the entire probe surface (according to the theory of piezoelectric phenomena electric signals at probe output are proportional to the aforementioned average value)

$$P_E(t) = \frac{1}{S} \int\limits_{S(\mathbf{x})} P^{\mathrm{sc}}(S(\mathbf{x}), t) Ap(S(\mathbf{x})) \, \mathrm{d}S, \tag{9}$$

where $S(\mathbf{x})$ denotes a point on the transducer surface, S stands for the transducer surface area and $Ap(S(\mathbf{x}))$ is the apodization function for the transducer surface. In this study $P_E(t)$ is referred to as the echo. The RF signal $P_{\mathrm{RF}}(t)$ represents a single line of scanning and is calculated as follows:

$$P_{\mathrm{RF}}(t) = h(t) \otimes P_E(t), \qquad h = F^{-1}[H(n)], \tag{10}$$

where $H(n)$ is the calculated system transmittance.

4. Results

The experimental setup is shown in Fig. 1. The research was carried out for a pipe made of latex, with internal diameter of 5 mm and wall thickness of 1.25 mm. Both the wall thickness and pipe diameter were similar to the corresponding dimensions of the common carotid artery for people at the age of 20. The velocity of ultrasonic wave in the pipe wall was determined by ultrasonic measurements and amounted to 1.333 of the velocity in water. The investigations employed the VED ultrasonic apparatus. The frequency of the VED transmitter was 6.75 MHz. The ultrasonic probe was excited by an electric signal with length equal to one half of the signal period. The bandwidth of the receiver, determined for the level of -3 dB, was 2.37 MHz. The ultrasonic beam was focused in water medium, at the depth of 23 mm from the transducer surface (Fig. 2).

Pulses of the ultrasonic wave nearby the transducer surface and in the focus are shown in Fig. 2. The pulses were measured by means of the hydrophone of the type: Sonic Technologies Model 800 Bilaminar Hydrophone.
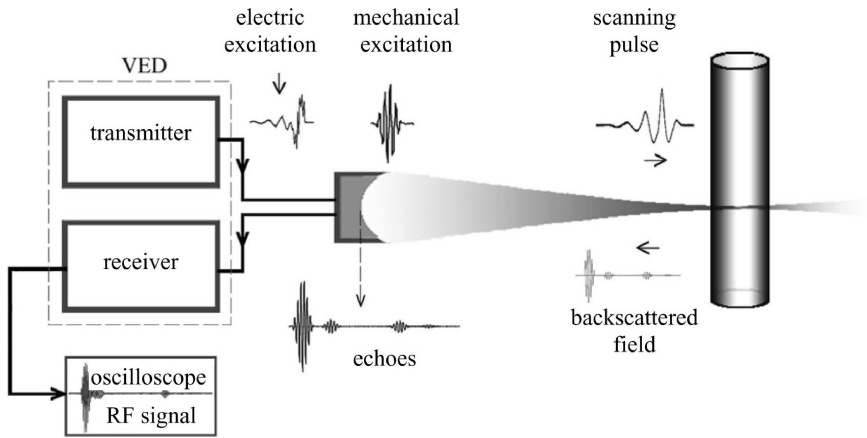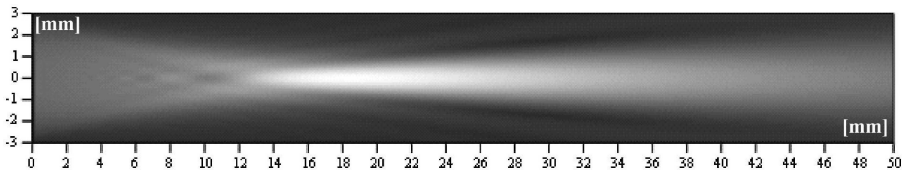

Fig. 1. Experimental setup.

Fig. 2. Numerically calculated Fourier component for the incident field, corresponding to the frequency of 6.5 MHz. The centre of the pipe coincides with beam axis within the distance of 26.75 mm.

During the performed research, the front surface of the pipe wall was located in the focus of the ultrasonic probe. The RF electric signal, $P_{\mathrm{RF}}(t)$, corresponding to echoes reflected by the pipe walls, was recorded at the output of the RF receiver by means of the digital oscilloscope AGILENT 54641D.
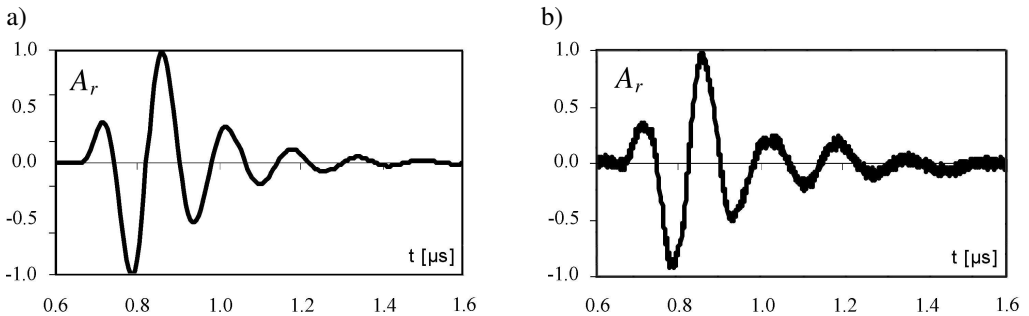
a)

b)

Fig. 3. a) The assumed normalized mechanical stimulation; b) the measured normalized mechanical stimulation, $A_r = P/P_0$, where P – pressure, $P_0 = 0.25$ MPa.

To highlight the relationships between the target (pipe) dimensions and wavelength of the echoed signals (both the acoustic wave and the corresponding electric waveforms), the scales were converted all the time into 3D ones and expressed in millimetres. Signal amplitudes were presented as relative values. Spatial size of the measurement "window" was 30 mm.

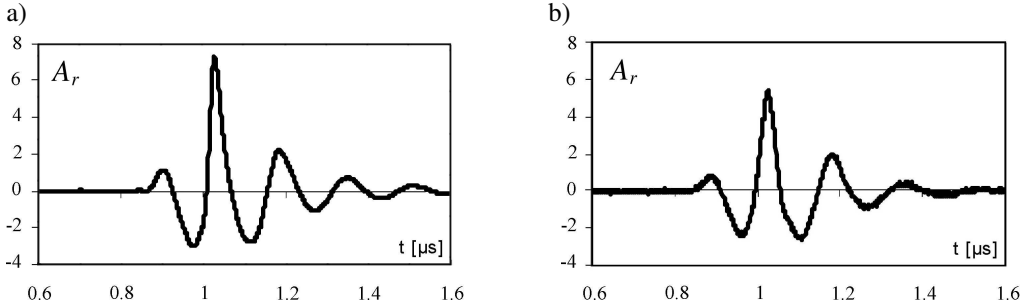Results for calculations and measurements are presented in Figs. 2–8.

a)

b)

Fig. 4. The normalized scanning pulse in the focus: a) calculated from the numerical model by means of the formula (8); b) the normalized scanning pulse measured in the focus, $A_r = P/P_0$, where P – pressure, $P_0 = 0.25$ MPa.
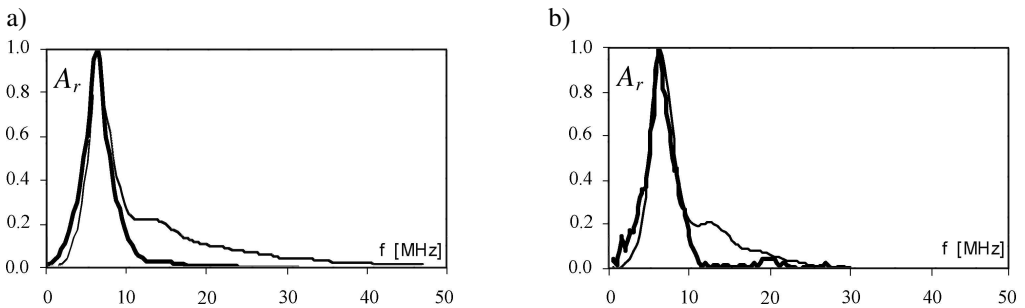
a)

b)

Fig. 5. a) The normalized spectrum of the assumed mechanical stimulation (thick line) and the normalized spectrum of the calculated scanning pulse in the focus (thin line); b) The normalized spectrum of the measured mechanical stimulation (thick line) and the normalized spectrum of the measured scanning pulse in the focus (thin line). A_r – the relative amplitude of the signal spectrum (with respect to the maximum value of the amplitude of spectrum).
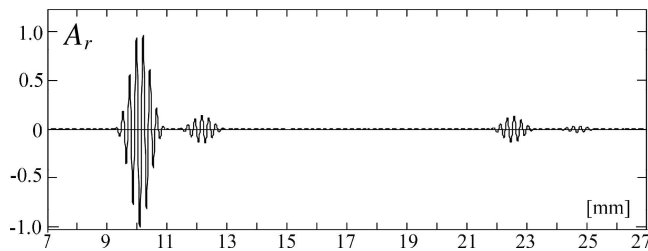
Fig. 6. Echo calculated from the numerical model by means of the formula (9). The point 16.5 on the scale above corresponds to location of the pipe centre at the distance of 26.75 mm from the ultrasonic probe, A_r – the relative amplitude (with respect to the maximum value of the echo amplitude).
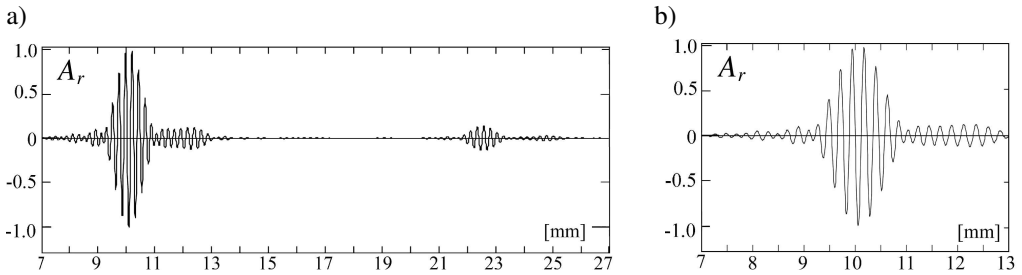
a)

b)

Fig. 7. a) The RF signal $(P_{\mathrm{RF}}(t))$ calculated from the numerical model by means of the formula (10); b) the expanded RF signal from the first pipe wall, A_r – the relative amplitude (with respect to the maximum value of the RF signal amplitude).

a)

b)

Fig. 8. a) The RF signal $(P_{\mathrm{RF}}(t))$ measured by means of the VED apparatus; b) the expanded RF signal from the first pipe wall, A_r – the relative amplitude (with respect to the maximum value of the RF signal amplitude).
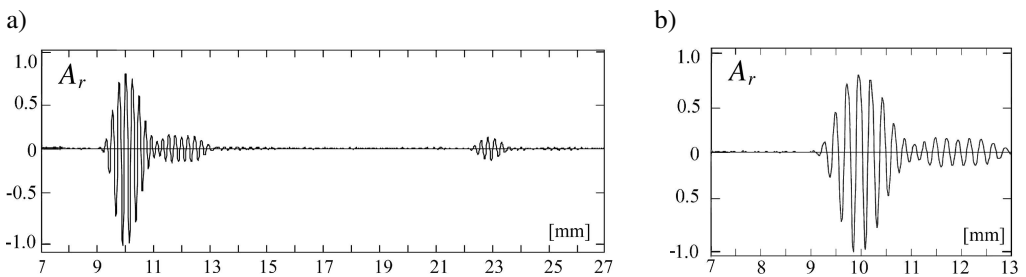
It is observed the decreasing of the amplitude of the scanning pulse measured in the focus (Fig. 4b) in comparison to the scanning pulse in the focus (Fig. 4a) calculated from the numerical model by means of the formula (8). This effect is due to the influence of the frequency characteristic and influence of the integrating limited surface of the active part (0.5 mm^2) of the applied hydrophone.

5. Conclusions

Comparison between the results that were obtained from numerical calculations and from measurements (Figs. 3–8) serves as a proof that the numerical model which has been developed enables simulation of the experiments with a good coherence, which was the actual objective of the study. The limited bandwidth of the receiver not permit for observation the effect of the nonlinearity propagation of the incident wave then it is allowed to omit the nonlinear wave propagation effects and using a linear approached for the signal analysis. The developed solver makes is possible to acquire information about the ultrasonic signal on every stage of its processing, with consideration to transfer functions of all the components down the receiving path, i.e. the ultrasonic probe, RF amplifier, etc. It is the matter of high importance when the designing process of measurement equipment is to be optimized.

Acknowledgment

References

[1] PETERSON L. H., JENSEN R. E., PARNELL J., *Mechanical properties of arteries in vivo*, Circulation Research, **8**, 622–639 (1960).

[2] RILEY W. A., BARNES R. W., SCHEY H. M., *An approach to the non invasive periodic assessment of arterial elasticity in the young*, Preventive Medicine, **13**, 169–184 (1984).

[3] RENEMAN R., VAN MERODE T., HICK P., MUTYTJENS A. M. M., HOEKS A. P. G., *Age related changes in carotid artery wall properties in men*, Ultrasound in Med. and Biol., **12**, 465–471 (1986).

[4] VAN MERODE T., BRANDS P. J., HOEKS A. P. G., RENEMAN R. S., *Faster ageing of the carotid artery bifurcation in borderline hypertensive subjects*, Journal of Hypertension, **11**, 171–176 (1993).

[5] POWAŁOWSKI T., PEŃSKO B., *A noninvasive ultrasonic method for the elasticity evaluation of the carotid arteries and its application in the diagnosis of the cerebro-vascular system*, Archives of Acoustics, **13**, 109–126 (1988).

[6] KAWASAKI T., SASAYAMA S., YAGI S., ASAKAWA T., HIRAI T., *Non-invasive assessment of the age related changes in stiffness of major branches of the human arteries*, Cardiovascular Research, **21**, 678–687 (1987).

[7] SZYMOŃSKI T., POWAŁOWSKI T., TRAWIŃSKI Z., ŁAPIŃSKI M., *Evaluation of the reproducibility of vascular echo Doppler system for the assessment of the carotid artery elasticity*, Acta Angiologica, **3**, 83–91 (1997).

[8] WÓJCIK J., *Conservation of energy and absorption in acoustic fields for linear and nonlinear propagation*, J. Acoust. Soc. Am., **104**, 2654–2663 (1998).

[9] WÓJCIK J., *Nonlinear reflection and transmission of plane acoustic waves*, Archives of Acoustics, **29**, 607–632 (2004).

[10] WÓJCIK J., NOWICKI A., LEWIN P. A., BLOOMFIELD P. E., KUJAWSKA T., FILIPCZYŃSKI L.[†], *Wave envelopes method for description of nonlinear acoustic wave propagation*, Ultrasonics, **44**, 310–329 (2006).